Numerical modelling of the non-isothermal flow of a non-Newtonian polymer in a co-kneader

L. Sardo, Bruno Vergnes, R. Valette

Numerical modelling of the non-isothermal flow of a non-Newtonian polymer in a co-kneader

L. Sardo, B. Vergnes, R. Valette*

MINES ParisTech, PSL Research University, CEMEF - Centre de Mise en Forme des Matériaux, UMR CNRS 7635, CS 10207, 06904 Sophia-Antipolis, France

*Corresponding author: R. Valette

rudy.valette@mines-paristech.fr

Abstract

The co-kneader is a particular single-screw extruder with pins fixed on the barrel, interrupted screw flights, and a screw with both rotational and reciprocating motions. The co-kneader is principally used for its excellent mixing capacities. In order to calculate the flow in the co-kneader, we developed a simplified Hele-Shaw model which takes into account the mixing pins and the reciprocating motion of the screw. In this paper we describe the model and the effects of the reciprocating motion and the presence of mixing pins on the polymer flow.

Keywords: co-kneader, extrusion, modelling, simulation, finite elements.

1. Introduction

The co-kneader is a particular single-screw extruder invented by Heinz List in 1947. It is commonly used for its excellent mixing capacities, specifically for the gelification of PVC compounds or the compounding of polymers highly filled with fibers, additives or carbon black. It is composed of a rotating single screw extruder, similar to a standard one, but with interrupted flights and mixing pins fixed to the barrel. The screw has also an axial reciprocal movement. These peculiarities make the flow of a molten polymer very complex , with a lot of separation and recombination of fluxes, explaining the mixing capacities of the machine. Moreover, as in twin-screw extrusion, the screw and the barrel are modular, thus enabling to adapt the configuration to the considered problem. Different types of elements are available. The most commonly used are the conveying and the mixing elements (Fig. 1). The conveying element is a single-flighted element with one flight interruption and one pin. The mixing element is a double-flighted element with three flight interruptions (on each flight) and six pins. Another specificity of the co-kneader is the so-called restriction ring, which allows to locally reduce the depth of the channel.

The determination of the best screw profile or the best processing conditions is thus a difficult task and is generally based on the experience of the user and on long and expensive trial and error procedures. Therefore, flow modelling appears as an interesting way to better understand the changes in temperature, pressure, and filling ratio along the screw, as well as the mixing efficiency for fixed processing conditions.

The first theoretical studies of the co-kneader were made by Booy and Kafka (1987) on a mixing section, using both lubrication approximations and 3D computations with Polyflow© software. Then, Brzoskowski et al. (1988) studied the flow in a pin-barrel extruder, i.e. a screw extruder with pins fixed onto the barrel, but without reciprocating motion. They used the 2D Flow Analysis Network (FAN) method. In the early nineties, Elemans and Meijer

(1990) developed a model which takes into account the pins but neglects the oscillating motion. They also performed experimental studies on a lab-scale co-kneader with a Plexiglas-barrel. A few years later, in a series of papers, Lyu and White (1995, 1996, 1997a-c, 2000) developed different 2D models, with the oscillating motion but without the mixing pins, complemented with experiments. They considered a non-Newtonian and non-isothermal behavior, and took into account the partial filling. In some papers, they considered also a viscoelastic behavior.

The previous studies concerned essentially 2 or 2.5D models that neglected either the mixing pins or the oscillation motion. More recently, full 3D simulations were proposed by Mehranpour et al. (2002, 2003), but without considering the pins. Until now, the most sophisticated full 3D model seems to be the one developed by Brito Bazan et al. (2012), based on the Finite Element method. It takes into account all the features of the co-kneader, except the partial filling. However, the calculation of this 3D model is very time-consuming and the selected mesh seems to be a little bit insufficient.

In the present paper, we present a global 2.5D model, based on the Hele-Shaw approximations, taking into account both the presence of mixing pins and the reciprocating motion of the screw.

2. Flow modelling

2.1 Usual approximations

In order to simplify the geometry and the kinematics of the co-kneader, some approximations commonly applied in single screw extrusion (Tadmor and Klein, 1970) will be used.

The first approximation is the channel unrolling, which consists on flattening the screw geometry. On a classical single screw, unrolling the channel is quite easy and the obtained geometry is a long parallelepiped. On the co-kneader, many interruptions of flights are present

and the channel width can vary according to the screw profile. The fact that the flight angle is different between the mixing and the conveying elements also increases the complexity of the unrolled geometry. In our case, we chose to unroll the geometry from the external diameter. For a specific configuration (two conveying elements followed by two mixing elements), we obtain the result shown in Figure 2. In the following, coordinate *x* will be parallel to the screw axis and *z* will be the transverse direction. By reason of symmetry, the polymer going out of the channels on the left side is re-entering on the right side at the same axial coordinate.

The second approximation is to consider the screw fixed and the barrel moving around the screw. In the unrolled configuration, the barrel is considered as a flat plane moving at the top of the channels with a velocity $\boldsymbol{V_B}$. It has two components, one in the transverse direction due to the rotation, $\boldsymbol{V_{Bz}}$, and one in the axial direction due to the reciprocating motion, $\boldsymbol{V_{Bx}}$:

$$\boldsymbol{V_B} = \boldsymbol{V_{Bz}} + \boldsymbol{V_{Bx}} = \omega \frac{D}{2} e_z + A\omega \sin \omega t \, e_x \qquad (1)$$

where ω is the rotation speed (in rad/s), D is the screw diameter, A is the amplitude of the oscillation, , and e_x and e_z are the components of the unit vector. The gap between the screw flights and the barrel is neglected.

2.2 Mechanical model

The flow in the co-kneader can be modelled using the Hele-Shaw approximations, in which the flow is locally considered as between parallel plates. Indeed, the depth of the channel is constant, except in the restriction ring element, and the polymer flows essentially in the *x* and *z*-directions. If we neglect inertia and gravity terms, the Stokes equations for a Newtonian fluid reduce to:

$$\frac{\partial p}{\partial x} = \eta \frac{\partial^2 u}{\partial y^2} \qquad (2)$$

$$\frac{\partial p}{\partial z} = \eta \frac{\partial^2 w}{\partial y^2} \tag{3}$$

where η is the viscosity. By integrating twice Eqs. (2) and (3) with appropriate boundary conditions (no slip on the screw and on the barrel), we obtain the velocity components:

$$u(y) = \frac{\partial p}{\partial x}\frac{1}{2\eta}(y^2 - Hy) + \frac{V_{Bx} y}{H} \tag{4}$$

$$w(y) = \frac{\partial p}{\partial z}\frac{1}{2\eta}(y^2 - Hy) + \frac{V_{Bz} y}{H} \tag{5}$$

where H is the channel depth. Integrating the velocity equations with respect to the height leads to the flow rates by unit width:

$$q_x = \frac{\partial p}{\partial x}\frac{1}{12\eta}H^3 + \frac{V_{Bx} H}{2} \tag{6}$$

$$q_z = \frac{\partial p}{\partial z}\frac{1}{12\eta}H^3 + \frac{V_{Bz} H}{2} \tag{7}$$

The continuum equation writes:

$$\frac{dq_x}{dx} + \frac{dq_z}{dz} = 0 \tag{8}$$

In Eqs. (2) to (7), the polymer is considered as Newtonian, which is not the case in the reality. In order to take into account the variation of the viscosity with the shear rate, we calculate locally an equivalent viscosity from the local shear rate, using an appropriate law (power law or Carreau law, for example).

The average local shear rate $\bar{\dot{\gamma}}$ is calculated with the following equations:

$$\dot{\gamma}_{xy}(y) = \frac{\partial u}{\partial y} = \frac{\partial p}{\partial x}\frac{1}{\eta}(y - \frac{H}{2}) + \frac{V_{Bx}}{H} \tag{9}$$

$$\dot{\gamma}_{zy}(y) = \frac{\partial w}{\partial y} = \frac{\partial p}{\partial z}\frac{1}{\eta}(y - \frac{H}{2}) + \frac{V_{Bz}}{H} \tag{10}$$

$$\bar{\dot{\gamma}} = \sqrt{\frac{1}{H}\int_0^H \left(\dot{\gamma}_{xy}^2 + \dot{\gamma}_{zy}^2\right) dy} \tag{11}$$

2.3 Non-isothermal model

As the mechanical model is based on the Hele-Shaw approximation, the temperature is considered as constant across the channel depth, and this average temperature $\bar{T}$ is only function of *x* and *z*. The thermal balance to solve on the domain Ω is thus:

$$\int_\Omega \rho c_p \left(\frac{\partial \bar{T}}{\partial t} + u\frac{\partial \bar{T}}{\partial x} + v\frac{\partial \bar{T}}{\partial y}\right) d\Omega = \int_{\partial\Omega} h_T \left(T_w - \bar{T}\right) d\partial\Omega + \int_\Omega \eta \bar{\dot{\gamma}}^2 d\Omega \tag{12}$$

where ρ is the polymer density, c_p is the heat capacity, h_T is the heat transfer coeffcient, and T_w is the barrel temperature. The first term of the right-hand side takes into account the heat transfer with the barrel and the second term represents the dissipated power, where $\bar{\dot{\gamma}}$ is defined by Eq. (11). In the case of a lab-scale co-kneader, where the screw is not thermally regulated, the contact with the screw is supposed to be adiabatic. Otherwise, a second term of heat transfer similar to the first one should be added to account for the transfer with the screw.

3. Simulation

To solve the model on the entire co-kneader domain, we choose the finite element method for its ability to address complex geometries.

3.1 Finite element method

Introducing Eqs. (6) ande (7) in Eq. (8), we obtain the following equation:

$$\nabla.\left(\frac{H^3}{12\eta}\nabla P\right) - \nabla.\left(\frac{\boldsymbol{V_B} H}{2}\right) = 0 \tag{13}$$

It is solved on the entire domain, using a finite element method with a linear discretization. The usually imposed boundary conditions to the system are a pressure at the exit and a flow rate at the entrance. The pressure is imposed by a Dirichlet condition, and the flow rate is imposed by a Neumann condition, i.e. that we impose in fact a pressure gradient: we solve Eq. (6) on the entrance boundary to obtain the desired pressure gradient.

The domain is "open" on the left and the right sides. To create the mesh, we thus need to obtain points at the same *x*-coordinates on both sides. Figure 3 shows an example of the mesh for the configuration of Figure 2.

The solution of Eq. (13) provides the pressure field in the whole domain, from which we calculate the pressure gradient in each element. Then, we can calculate the velocities, the shear rates (and thus the viscosity) using Eqs. (4) to (11).

The thermal balance (Eq. (12)) is also solved by a finite elements method, with a SUPG (Streamline Upwind Petrov-Galerkin) formulation to limit the numerical diffusion of the transport term (Johnson et al., 1984).

3.2 The oscillating motion

The co-kneader has a reciprocating motion. The oscillating speed is not negligible as we can see in Figure 4: for a lab-scale co-kneader (diameter D = 30 mm), at 300 rpm, it varies between – 10.5 and 10.5 cm/s, for a rotational speed of 47.1 cm/s at the barrel. To observe the impact of the oscillation on the flow rate, we performed some simulations by imposing the atmospheric pressure at both ends of the domain shown in Figure 5. It represents a part of the lab-scale co-kneader configuration and is constituted by two conveying elements in series with two mixing elements and a restriction ring. We observe in Figure 6 that the calculated flow rate also oscillates, with the same frequency as the axial velocity, and we can see that the flow is strongly affected by the reciprocating motion. In order to simulate realistic processing

conditions, we need to impose a flow rate through the co-kneader. We first tried to impose a fixed flow rate Q_{imp}. As explained before, it is equivalent to impose a pressure gradient defined as:

$$\frac{\partial P(t)}{\partial x} = \frac{6\eta V_{Bx}(t)}{H^2} - \frac{12\eta}{H^3 W} Q_{imp} \tag{14}$$

where W is the width of the flow domain. As we can see from Eq. (14), the pressure gradient at the entry of the domain is now varying with time. We observe in Figure 7 the impact of the barrel oscillation on the pressure profile during a rotation: the pressure at the entrance varies of several MPa (from -3.2 to 1.2 MPa, in the case considered, i.e. 300 rpm and xx kg/h). Moreover, the filled length (represented by the zero value of the pressure) varies also in an unrealistic way (in the chosen conditions, the duration of one oscillation is 0.2 s). We thus need to impose the flow rate differently. We tested in a second step to impose a flow rate oscillating with time, with the same average value Q_{imp}. Now, the entry pressure gradient is constant:

$$\frac{\partial P}{\partial x} = -\frac{12\eta}{H^3 W} Q_{imp} \tag{15}$$

and the flow rate oscillates, according to :

$$Q(t) = Q_{imp} + \frac{V_{Bx}(t) HW}{2} \tag{16}$$

The results of this second method are similar to the previous ones and are also totally unrealistic. Therefore, the way to impose a flow rate during the reciprocating motion of the screw appears as a major issue that, to our knowledge, has never been addressed in the literature.

As explained before, a screw profile is usually made with two main kinds of screw elements: the conveying elements and the mixing elements. If we compare the flow rate during an

oscillation of the selected screw profile (Fig. 5), obtained by imposing a zero pressure at both ends, to the flow rate obtained in the same conditions on the conveying and mixing elements, we see in Figure 8 that the flow rate of the conveying element is close to the flow rate of the selected screw profile. Therefore, we propose to impose an oscillating flow rate, with an average value equal to $Q_{imp,}$ and an amplitude of oscillations corresponding to those of a conveying element at the same screw speed: the curve of Figure 8 is simply shifted vertically to impose the desired value of Q_{imp}. The pressure map obtained for the two extreme positions during one oscillation is shown in Figure 9. We only show the positive pressures, corresponding to the filled part of the co-kneader. We observe that the global pressure gradient changes from negative when the screw moves backwards to positive when it moves forwards, as already shown by Lyu and White (1996) with a model based on the FAN method. This impacts the filling length which is more important when the screw is back.

3.3 The mixing pins

Until now, we have not considered the presence of the mixing pins. In the moving barrel assumption, as they are fixed on the barrel, they are also moving with time. To take them into account, we add to the initial mesh the trajectory of the mixing pins given by the barrel speed (Eq. (1)) and we refine the mesh around these trajectories (Fig. 10). Then we determine the position of the mixing pins at each time of the simulation. We also impose their speed equal to the barrel speed.

We performed some simulations by imposing the screw speed and the atmospheric pressure at each extremity of the flow domain. We can see in Figure 11 that the curves of the flow rate evolution during one rotation, with or without mixing pins, are very close. The presence of mixing pins does not modify the global flow rate. Similar results have been experimentally verified by Yabushita et al. (1989) on a pin barrel extruder.

If we zoom on a mixing pin (Fig. 12), we can see that, when it is close to the screw flight, the shear rate is much higher than in the channel. In the example shown here (at 500 rpm), the maximum shear rate is around 1100 s^{-1}, when it is only around 150 s^{-1} in the screw channel. This high shear rate is responsible of the efficiency of the co-kneader for dispersive mixing.

4. Examples of results

The screw profile used in this section is the one shown in Figure 5. As we saw previously that the mixing pins do not change the relationships between pressure and flow rate, they are neglected in the following results. The reciprocating motion affects the flow but it is quite complicated to present results varying with time during the oscillating motion. Therefore we choose to present results without oscillations, which represent an average of the flow conditions during one rotation.

The pressure change along the screw profile at constant screw speed (250 rpm) and for various flow rates (2.5 to 7 kg/h) is shown in Figure 13. We observe that the pressure is negative in the major part of the profile, indicating that the co-kneader is only very partially filled. If we focus on the positive values, corresponding to the zone where the screw is totally filled, we can see in Figure 14 that the pressure is maximum at the entry of the restriction ring. It increases gradually with the flow rate. As the pressure gradient is lower with the increasing flow rate, this induces a longer filled length: it increases from 20 to 35 and 65 mm when the flow rate changes from 2.5 to 5 and 7 kg/h. All these results are qualitatively in agreement with the experiments of Elemans and Meyer (1990).

We performed the same simulation but with a fixed flow rate (7 kg/h) and various screw speeds. We can see in Figure 16 that the pressure in the last part of the restriction ring is the same regardless the speed. However, it increases slightly in the converging part. The pressure gradient increases with the screw speed, inducing also a longer filed section when the screw

speed is low: 22 mm at 450 rpm, 32 mm at 350 rpm and 60 mm at 250 rpm.Once again, these results are in coherence with the experimentation (Elemans and Meyer, 1990).

Finally, we show in Figure 17 the average temperature field obtained for 450 rpm and 11 kg/h, with an entry temperature and a barrel temperature of 180°C. The temperature field is very homogeneous, with an increase by viscous heating in the first conveying elements, followed by a stabilization around 205°C. This kind of flat profile was also obtained theoretically by Elemans and Meijer (1990) and Lyu and White (1997c), and experimentally confirmed by the latter.

5. Conclusions

In this paper, we have developed a non-Newtonian and non-isothermal 2.5D model based on the Hele-Shaw approximations for calculating the flow in a co-kneader. The model includes the two major specificities of the co-kneader, i.e. the presence of mixing pins and the reciprocating motion. We showed that the mixing pins only affect locally the shear rate and do not modify the pressure/flow rate relationships. On the opposite, the oscillating motion strongly affects the pressure profile. We have put in evidence the difficulty to impose a selected flow rate when the reciprocating motion is taken into account. The obtained results show that the model correctly describes the effects of varying screw speed and feed rate. However, the partial filling of the co-kneader is not yet considered. This point is actually in progress through the development of a level-set approach (Sardo, 2016).

Acknowledgements

This work has been carried out throughout the project LUCOMAX, funded by the French National Research Agency(ANR).

References

Booy, M. L. and Kafka, F.Y., "Isothermal flow of viscous liquids in the mixing section of a Buss kneader", SPE ANTEC Tech. papers, 140–145 (1987).

Brito-Bazan, M., Fradette, L. and Tanguy, P. A., “Experimental flow visualization and residence time distributions in a co-kneader”, Intern. Polym. Proc., **27**, 414–426 (2012).

Brzoskowski, R., White, J. L., Szydlowski, W., Nakajima, N. and Min, K., "Modelling flow in pin-barrel screw extruders", Intern. Polym. Proc., **3**, 134–140 (1988).

Elemans, P. H. M. and Meijer, H. E. H., "On the modeling of continuous mixers. Part II: The co-kneader", Polym. Eng. Sci., **30**, 893–904 (1990).

Johnson, C., Nävert, U. and Pitkäranta, J., “Finite element methods for linear hyperbolic problems”, Comput. Meth. Appl. Mech. Eng., **5**, 285-312 (1984).

List, H., Swiss patent 247,704, (1947) Lyu, M.-Y. and White, J. L., "Models of flow and experimental studies on a modular List/Buss kokneter", Intern. Polym. Proc., **10**, 305–313 (1995).

Lyu, M.-Y. and White, J. L., “Modelling of a viscous non-Newtonian polymer melt in a List/Buss kneader and comparison to experiment”, Intern. Polym. Proc., **11**, 208–221 (1996).

Lyu, M.-Y. and White, J. L., "Non-isothermal non-Newtonian analysis of flow in a modular List/Buss kneader", J. Reinf. Plast. Compos., **16**, 1445–1460 (1997a).

Lyu, M.-Y. and White, J. L., "Simulation of linear viscoelastic flow behavior in the Buss kneader", Polym. Eng. Sci., **37**, 623–635 (1997b).

Lyu, M.-Y. and White, J. L., "Simulation of non-isothermal flow in a modular Buss kneader and comparison with experiment", Intern. Polym. Proc., **12**, 104–109 (1997c).

Lyu, M.-Y. and White, J. L., "Simulation of non-linear viscoelastic flow behavior in the Buss kneader", J. Reinf. Plast. Compos., **19**, 756–791 (2000).

Mehranpour, M., Nazokdast, H. and Dabir, B., " Computational study of the velocity field in the conveying element of a ko-kneader with CFD method", Intern. Polym. Proc., **17**, 108–114 (2002).

Mehranpour, M., Nazokdast, H. and Dabir, B., " Computational study of velocity field in the KE element of a modular ko-kneader with CFD method", Intern. Polym. Proc., 18, 330–337 (2003).

Sardo, L., "Modélisation et simulation numérique de la thermodynamique des écoulements dans les co-malaxeurs", PhD dissertation, PSL Research University (2016).

Tadmor, Z. and Klein, I., Engineering Principles of Plasticating Extrusion. Van Nostrand Rheinhold, New York (1970).

Yabushita, Y., Brzoskowski, R., White, J. L. and Najakima, N., "Flow of rubber compound in a pin barrel screw extruder", Intern. Polym. Proc., **4**, 219–224 (1989).

Figure captions

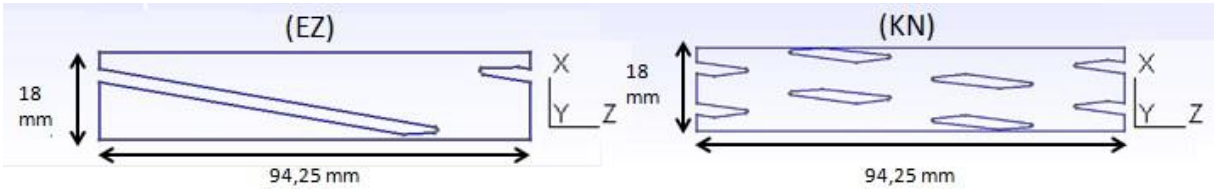

Figure 3. Unrolled representation of the conveying (EZ) and mixing (KN) elements of a lab-scale co-kneader

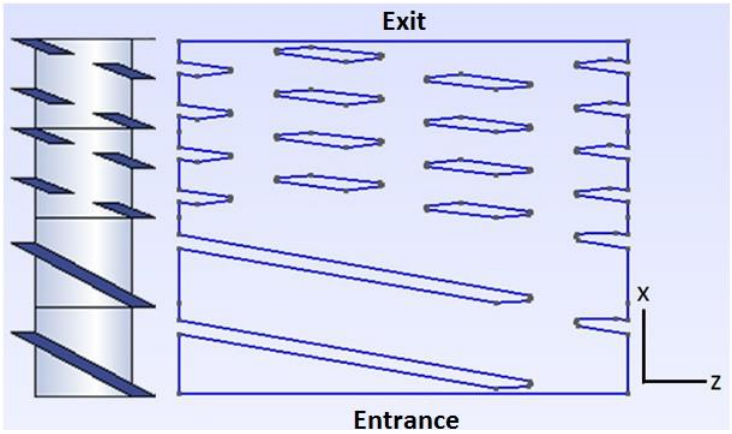

Figure 4. Unrolled screw section of a co-kneader (2 conveying and 2 mixing elements)

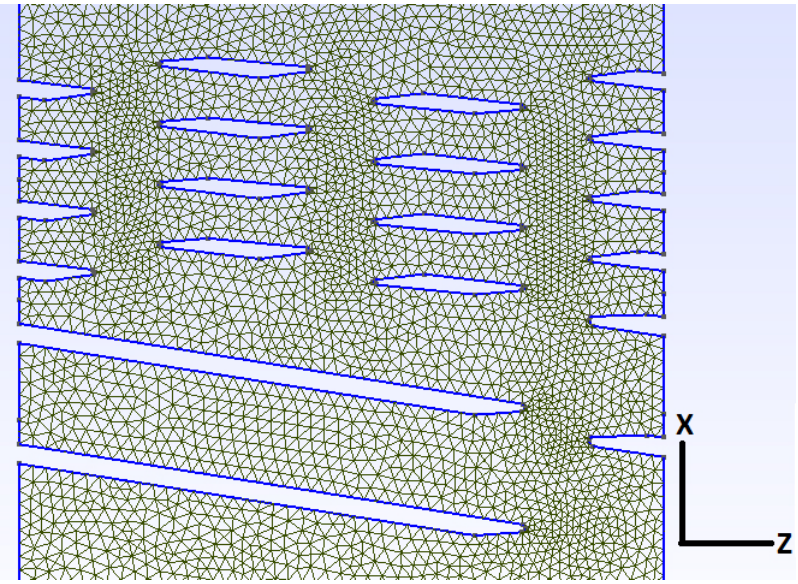

Figure 3. Finite element mesh of the flow domain of Fig. 2

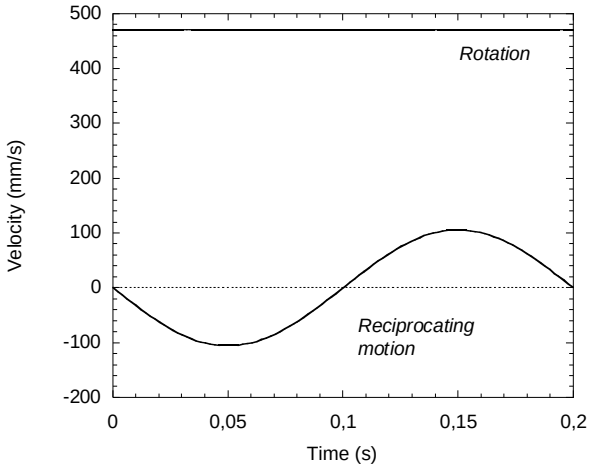

Figure 4. Rotational and reciprocating velocity during one rotation at 300 rpm (lab-scale co-kneader with a diameter of 30 mm)

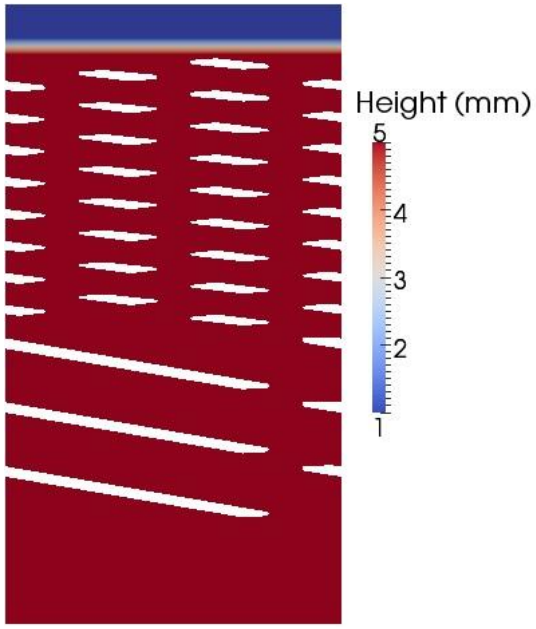

Figure 5. Screw configuration used in the calculations. The flow is from bottom to top. The blue zone is the restriction ring

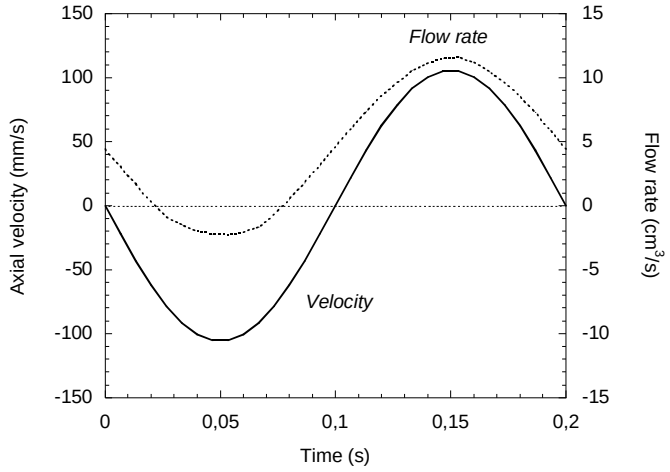

Figure 6. Oscillations of flow rate and axial velocity during one rotation at 300 rpm (lab-scale co-kneader with a diameter of 30 mm)

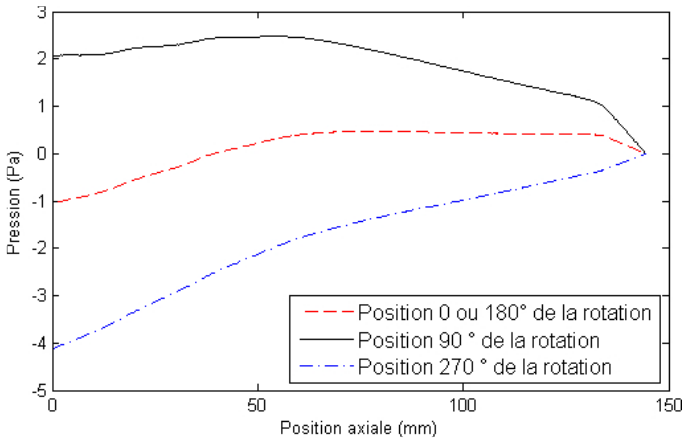

Figure 7. Pressure evolution along the flow domain during one rotation at 300 rpm (90° corresponds to the backward position of the screw, 270° to the forward one)

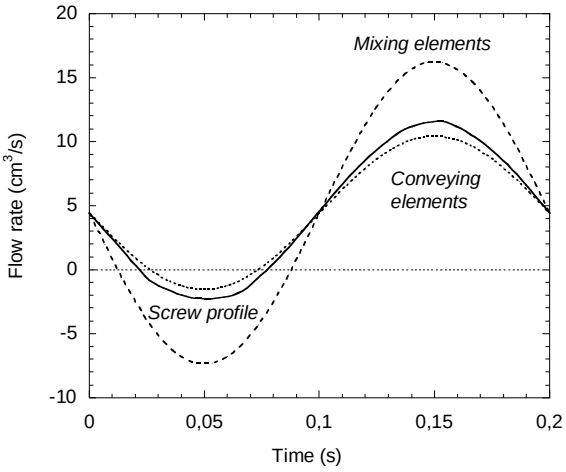

Figure 8. Oscillations during one rotation (at 300 rpm) of the flow rates of the selected screw profile (─), the mixing elements (--) and the conveying elements (···)

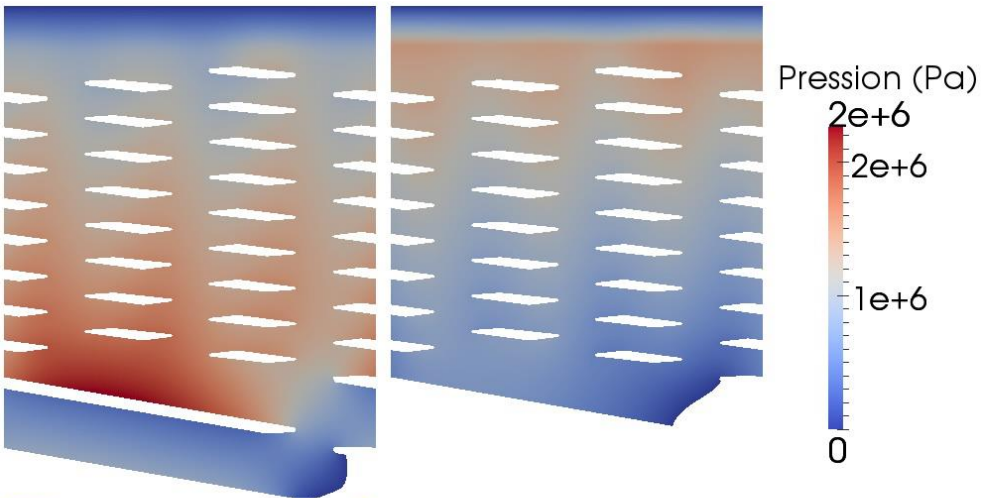

Figure 9. Pressure map into the flow domain for the two extreme positions of the screw (300 rpm, xx kg/h)

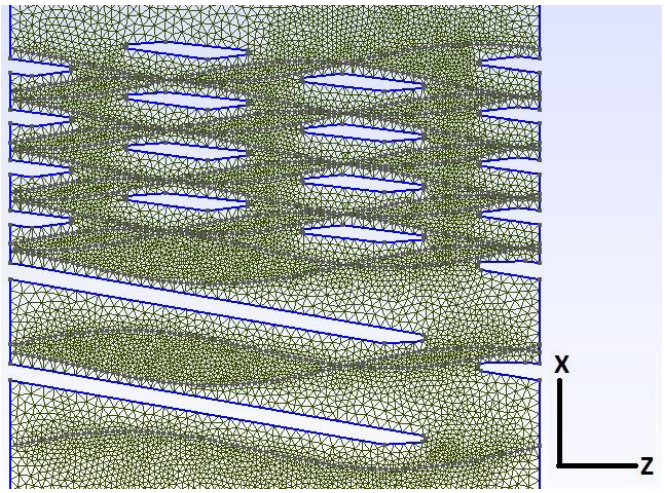

Figure 10. Finite element mesh of the flow domain including the trajectories of the mixing pins

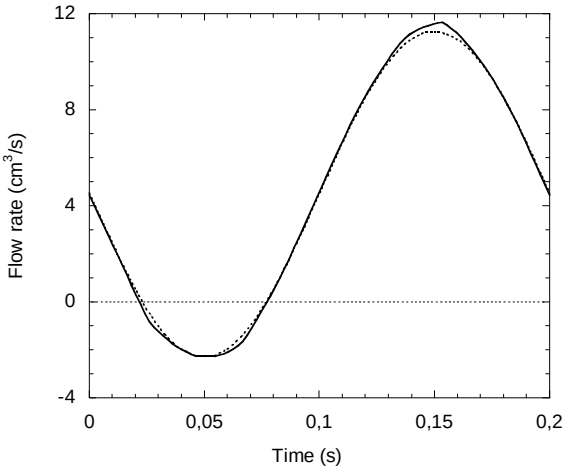

Figure 11. Oscillations of the flow rate during one rotation in the geometry of Fig. 5, with (─) and without (···) mixing pins

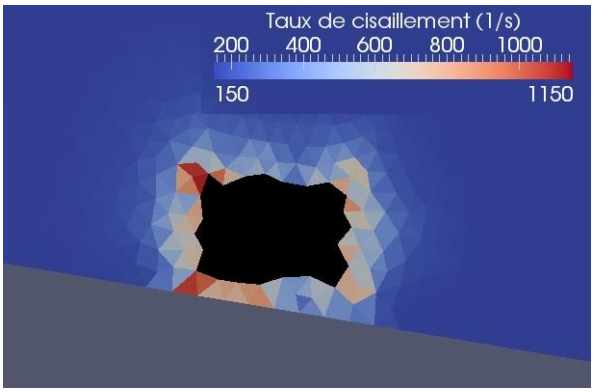

Figure 12. Shear rates around a mixing pin at 500 rpm

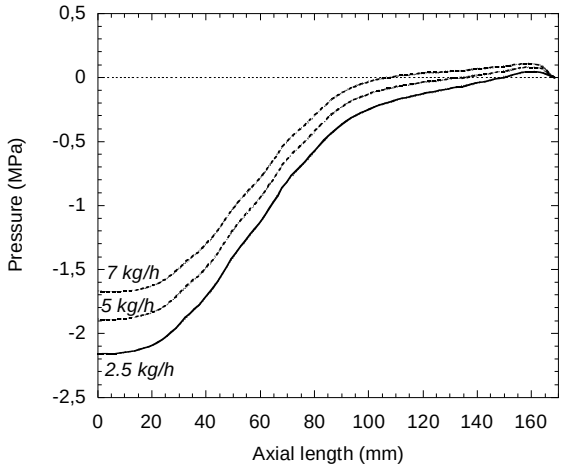

Figure 13. Pressure profiles along the screw for various flow rates at 250 rpm

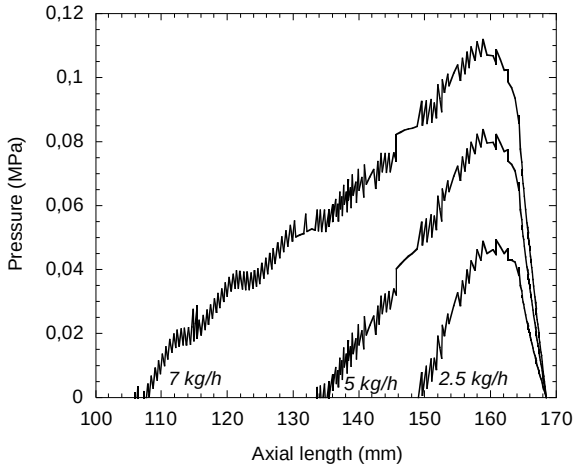

Figure 14. Pressure profiles along the filled part of the screw for various flow rates at 250 rpm

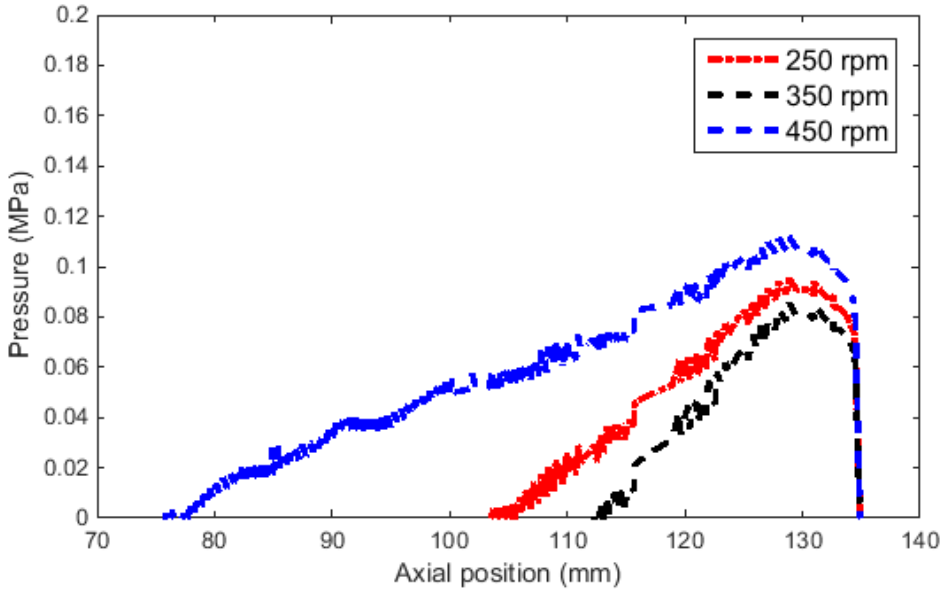

Fig. 16: Pressure profile for different screw speeds at 7 kg/h

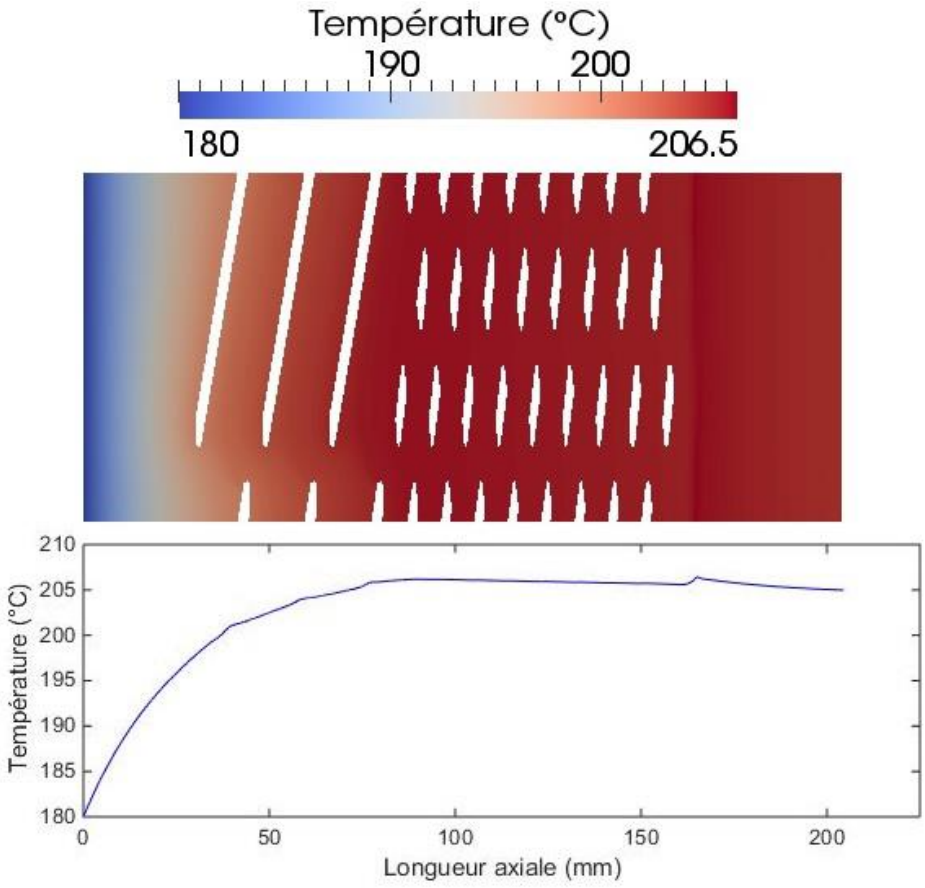

Fig. 17: Average temperature field at 450 rpm and 11 kg/h and temperature profile along the flow domain